Native Top-Down ESI-MS of 158 kDa Protein Complex by High Resolution Fourier Transform Ion Cyclotron Resonance Mass Spectrometry.

ARTICLE *in* ANALYTICAL CHEMISTRY · DECEMBER 2013

Impact Factor: 5.64 · DOI: 10.1021/ac4033214 · Source: PubMed

4 AUTHORS, INCLUDING:

Huilin Li

University of California, Los Angeles

24 PUBLICATIONS **361** CITATIONS

SEE PROFILE

analytical chemistry

Letter

pubs.acs.org/ac

Native Top-Down Electrospray Ionization-Mass Spectrometry of 158 kDa Protein Complex by High-Resolution Fourier Transform Ion Cyclotron Resonance Mass Spectrometry

Huilin Li,[†] Jeremy J. Wolff,[§] Steve L. Van Orden,[§] and Joseph A. Loo*[,†,‡]

[†]Department of Biological Chemistry, David Geffen School of Medicine and [‡]Department of Chemistry and Biochemistry, University of California, Los Angeles, California, 90095, United States

[§]Bruker Daltonics, 40 Manning Road, Billerica, Massachusetts, 01821, United States

Supporting Information

ABSTRACT: Fourier transform ion cyclotron resonance mass spectrometry (FTICR MS) delivers high resolving power, mass measurement accuracy, and the capabilities for unambiguously sequencing by a top-down MS approach. Here, we report isotopic resolution of a 158 kDa protein complex, tetrameric aldolase with an average absolute deviation of 0.36 ppm and an average resolving power of ~520 000 at m/z 6033 for the 26+ charge state in magnitude mode. Phase correction further improves the resolving power and average absolute deviation by 1.3-fold. Furthermore, native top-down electron capture dissociation (ECD) enables the sequencing of 168 C-terminal amino acid (AA) residues out of 463 total AAs. Combining the data from top-down MS of native and denatured aldolase complexes, a total of 56% of the total backbone bonds were cleaved. The observation of complementary product ion pairs confirms the correctness of the sequence and also the accuracy of the mass fitting of the isotopic distribution of the aldolase tetramer. Top-down MS of the native protein provides complementary sequence information to top-down ECD and collisionally activated dissociation (CAD) MS of the denatured protein. Moreover, native top-down ECD of aldolase tetramer reveals that ECD fragmentation is not limited only to the flexible regions of protein complexes and that regions located on the surface topology are prone to ECD cleavage.

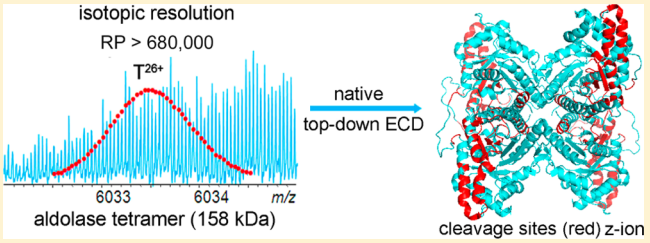

An emerging technique, "native" mass spectrometry (MS), has been successfully used to characterize intact, noncovalently bound protein complexes, providing stoichiometry and structural information that is complementary to data supplied by conventional structural biology techniques.[1−3] To confidently characterize protein complexes, electrospray ionization (ESI)-MS measurements acquired with isotopic resolving power (RP) and high mass accuracy and capabilities for deriving primary structure, i.e., sequence, information would be ideal. Fourier transform ion cyclotron resonance mass spectrometry (FTICR MS) is prominent for its superior resolving power and mass accuracy and its utility for tandem MS (MS/MS) with a variety of fragmentation techniques; FTICR MS is noted for characterizating posttranslational modifications (PTMs) and protein−ligand and protein−protein interactions.[4−9] However, it remains challenging to isotopically resolve large biomolecules over 100 kDa due to sample heterogeneity, cation/solvent/buffer addition, space charge effects, and electric and magnetic field inhomogeneity (for FTICR).[10−13] Unit mass resolution has been achieved for a few *denatured* proteins, including a 112 kDa protein with 3 Da mass error using a 9.4 T FTICR MS,[14] a 115 kDa protein by a 7 T instrument with a mass error of 5 ppm,[4] and a 148 kDa protein with a mass error of 1 Da by a 9.4 T FTMS.[10]

Compared to denatured proteins, it is more difficult to achieve isotopic resolution for inherently lower charged (and thus, higher m/z) native protein complexes because (1) the peak height is proportional to its charge state, (2) the resolving power is inversely proportional to mass-to-charge ratio for FTICR MS, and (3) the broader isotope distribution of large biomolecules reduces overall signal-to-noise ratio.[15] However, the introduction of a new FTICR analyzer cell, the ParaCell, by Nikolaev and co-workers has significantly increased the resolving power of FTICR MS.[16,17] By dynamically harmonizing the electric field potential at any radius of cyclotron motion in the entire cell volume, a resolving power of 39 M has been achieved for the alkaloid, resperine (m/z 609), using a 7 T system.[18] In addition, a few native protein complexes, including enolase dimer (93 kDa, RP ~ 800 000 at m/z 4250), alcohol dehydrogenase tetramer (147 kDa, RP ~ 500 000 at m/z 5465), and enolase tetramer (186 kDa), have been isotopically resolved with a 12 T FTICR system with the new ICR cell.[18] Although Mitchell and Smith reported that cyclotron phase locking due to Coulombic interactions limits the highest mass

Received: October 14, 2013
Accepted: December 6, 2013
Published: December 6, 2013

   dx.doi.org/10.1021/ac4033214 | *Anal. Chem.* 2014, 86, 317−320

that unit mass resolution can be achieved by FTICR MS ($M_{max} \approx (1 \times 10^4)B$, where B is magnetic field strength),[19] the ParaCell has made it significantly easier and promising to measure high-resolution mass spectra for large native protein complexes.

Another advantage of FTICR MS is its capability to employ a variety of fragmentation techniques, especially for top-down MS analysis, including in-source dissociation (ISD), collisionally activated dissociation (CAD), electron transfer dissociation (ETD), electron capture dissociation (ECD), electron detachment dissociation (EDD), and infrared multiphoton dissociation (IRMPD). Therefore, for the characterization of large proteins and protein complexes, beyond accurately measuring molecular masses (and thereby providing information on complex stoichiometry), further structural information (e.g., amino acid sequence, point mutations, metal binding sites, identification, and quantification of subunit variants) can be obtained.[5,6,8]

Here, we report subparts-per-million (ppm) mass accuracy with isotopic resolution of a 158 kDa protein complex (aldolase homotetramer) using FTICR MS with a dynamically harmonized cell. Top-down MS analyses confirm the sequence and also the accuracy of the mass fitting of the isotopic distribution of the protein tetramer. In addition, native top-down ECD analysis of the protein complex reveals that ECD fragmentation is not limited to only the flexible regions of protein structure, and it also demonstrates that native top-down ECD provides complementary sequence information to top-down ECD and CAD of denatured proteins.

EXPERIMENTAL METHODS

High-resolution measurements for the native protein solutions were acquired using a 12 T Bruker solariX XR FTICR MS (Bruker Daltonics, Bremen, Germany) with the ParaCell. Other experiments were performed using a 15 T Bruker solariX FTICR MS with an infinity cell (see the Supporting Information for more details.)

RESULTS AND DISCUSSION

Isotopically Resolved Aldolase Tetramer (~160 kDa). Fructose-1,6-bisphosphate aldolase (aldolase; EC 4.1.2.13) catalyzes the cleavage of fructose 1,6-bisphosphate to yield dihydroxyacetone phosphate (DHAP) and glyceraldehyde 3-phosphate in glycolysis. Aldolases are homotetrameric complexes, with each subunit having an architecture with a $(\alpha/\beta)_8$-barrel fold. The aldolase protein subunit from rabbit muscle is composed of 363 amino acids and an average mass of ~39 211 Da, and its corresponding homotetramer complex has a calculated mass of 156 845 Da.

Figure 1A shows the MS spectrum of aldolase tertramer under native nanoESI conditions using a 12 T FTICR MS with the ParaCell analyzer. A relatively narrow charge state distribution (29+ to 25+) was observed between m/z 5400 and 6300. Five isotopic "beats" were observed for the time-domain acquisition period (36 s) with a beat period of 5.1 s (Figure 1B). The relatively long beat period makes the achievement of ultrahigh resolving power very challenging because of space charge effects, and electric and magnetic field inhomogeneity can induce frequency shifts during a long transient period, leading to signal decay.[11,12] Using our 15 T FTICR MS with an infinity cell, only 3 isotopic "beats" were observed for measurements of the isolated 27+ charge state

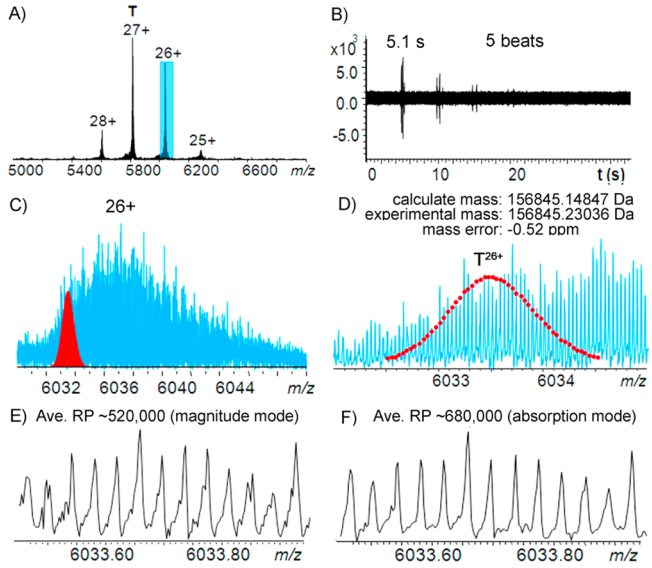

Figure 1. Native ESI-mass spectrum of aldolase tetramer with a 12 T FTICR MS with a ParaCell. (A) Full mass spectrum of aldolase tetramer, (B) corresponding time-domain transient acquired for aldolase tetramer, (C) the expanded MS spectrum of the 26+ charge state of aldolase tetramer with the theoretical isotopic distribution for the 26+ nonadducted aldolase tetramer $[(C_{1733}H_{2773}N_{489}O_{525}S_{11})_4 + 26H]^{26+}$ in red, (D) expanded spectrum of part C, and (E) expanded mass spectra in magnitude mode and (F) in absorption mode.

ions at m/z 5820 (isolated with a mass window of ±50 Da to minimize ion cloud interactions), which is insufficient for achieving isotopic resolution (Figure S-1 in the Supporting Information). The ParaCell significantly improves the ability to collect long transients, however, by dynamically harmonizing the electric field potential at any radius of cyclotron motion in the cell, thus making isotopic resolution of larger molecules achievable.[16,20]

Figure 1C shows the expanded mass spectrum for the 26+ charge state ions, and it can be seen that the analyte peaks span over 20−100 Da, likely due to a combination of sample heterogeneity, neutral losses, and cation/buffer/solvent adduction, which makes the isotopic mass fitting of the aldolase tetramer challenging. To confirm the accurate molecular weight, aldolase was denatured with acetonitrile−H_2O−formic acid (49.95/49.95/0.10) (see Figure S-2 in the Supporting Information) and measured by nanoESI-MS. Taking the 26+ charged aldolase monomer as an example, the peak at m/z 1509 fits the theoretical mass of aldolase A (from rabbit muscle) with an mass error of 0.7 ppm and a series of sodium adduct peaks were also observed at higher m/z. Top-down CAD and ECD experiments were further performed to confirm the sequence of aldolase from rabbit (*Oryctolagus cuniculus*) (UniProtKB/Swiss-Prot: P00883/ALDOA_RABIT) (Figure S-3 in the Supporting Information). The observation of a series of b/y and c/z$^\bullet$ product ions, particularly the complementary ion pairs, b_{183}^{15+}/y_{180}^{11+} (Figure S-3B in the Supporting Information inset) and c_{217}^{14+}/$z_{146}^{11+\bullet}$ (Figure S-3A in the Supporting Information inset), confirms that there are no PTMs or mutations present (at least above 5% relative abundance) and the elemental composition of the monomer is $C_{1733}H_{2773}N_{489}O_{525}S_{11}$. The isotopic distribution of the 26+ nonadducted aldolase tetramer $[(C_{1733}H_{2773}N_{489}O_{525}S_{11})_4 + 26H]^{26+}$ was then simulated to fit the experimental result (Figure 1C,D). As the molecular mass increases, the isotopic distribution widens and the peak

dx.doi.org/10.1021/ac4033214 | Anal. Chem. 2014, 86, 317−320

intensity of the monoisotope (i.e., all light isotopes) is reduced;[21] for the ~158 kDa aldolase tetramer, the monoisotopic peak is no longer observable. Therefore, the mass of the peak with the highest intensity is reported here, which is off by 0.081 89 Da compared to the calculated theoretical mass. An average absolute deviation of 0.36 ppm (Table S-1 in the Supporting Information) was achieved for the entire isotopic peak distribution of the nonadducted aldolase tetramer.

It has been demonstrated that phase correction can greatly improve resolving power, mass accuracy, and signal-to-noise for FTICR MS.[22−24] By correcting the phase using Bruker solariX XR software, an average mass resolving power of ~680 000 (Figure 1F) was achieved for the 26+ ion at m/z 6033 in absorption mode, which is 1.3-fold higher than the resolving power in magnitude mode (Figure 1E). In addition, peak shape becomes narrower and smoother after phase correction and the average absolute mass deviation improved by 1.3-fold (to 0.28 ppm).

Top-Down ECD of Aldolase Complex. One of the unique features of ECD is the preservation of labile bonds, including bonds associated with PTMs and noncovalent interactions, while cleaving backbone N−Cα bonds.[25] Thus, potentially ECD is a powerful tool to locate the noncovalent binding sites or interfaces of metal, ligand, or protein to their protein target.[6,8,26−28] Recently, Gross and co-workers proposed that the regions of a protein complex that fragment by native top-down ECD correlate with the "B-factor" of that protein, namely, ECD products originate from the flexible regions of a protein.[6]

The entire charge state envelope was subjected to ECD without prior ion selection due to the upper mass isolation limit (m/z ~6000) of the mass selective quadrupole. Skimmer 1 voltage was varied to preactivate ions and to improve ECD fragmentation efficiency. With a skimmer potential of 90 V, native ECD of aldolase tetramer starts to induce fragments from the amino acid (AA) 280−360 region (see Figure S-4 in the Supporting Information). Further increasing the skimmer potential to 120 V improves the ECD backbone cleavage efficiency. However, by increasing the skimmer potential to 150 V or even higher, although more fragments from the middle region of the sequence are generated, many of the fragments from AA 280−330 disappear, which suggests that a conformational change of the aldolase tetramer may have been induced. Figure 2A shows the top-down ECD mass spectrum of the aldolase tetramer with the skimmer potential of 120 V. Products ions resulting from cleavage of N−Cα bonds are found at m/z 3500 and below and are assigned with mass errors within ±5 ppm (Figure S-5 in the Supporting Information). No b/y product ions were induced during the preactivation, and most of the fragment ions are z$^\bullet$-ions from residues 211−363, except for two c-ions (c_7 and c_{22}) (shown in cyan, Figure 2B).

Native top-down CAD and ISD were also performed for the aldolase tetramer; dissociation of the tetramer to yield monomer was observed in both approaches and no sequence information was obtained. The cleavage sites from ECD (colored in red) and CAD (colored in green) of the denatured aldolase monomer (26+) are overlaid with the native ECD results for aldolase tetramer (Figure 2B). As shown in Figure 2B, in contrast to the limited number of c-ion fragments observed in the ECD of aldolase tetramer, ECD of denatured aldolase monomer induces extensive c-ion fragments in the N-terminal region and enables the assignment of first 156 N-terminal AA residues. Surprisingly, the number of z$^\bullet$-ions observed from ECD of the denatured aldolase monomer is much less compared to the ECD of the native aldolase tetramer. Although it may be possible that the z$^\bullet$-ions may undergo secondary fragmentation due to excess available energy, electrons, or long ion-electron reaction times during the ECD experiment, ECD experiments with reduced reaction time and bias voltages were performed and the results argue against this assumption. Overall, 56% of the total number of backbone bonds are cleaved from combining top-down MS of native aldolase complex and denatured aldolase monomer (23% for native ECD of aldolase tetramer, 37% for ECD of denatured aldolase, and 5% for CAD of denatured aldolase).

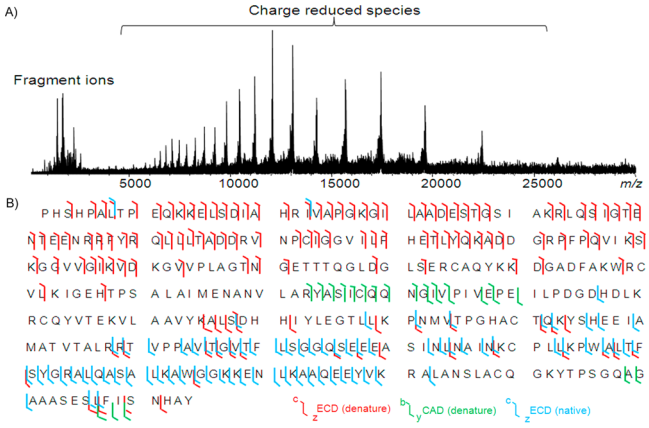

Figure 2. (A) Native top-down ECD mass spectrum of the aldolase tetramer and (B) backbone cleavage coverage of aldolase by top-down MS/MS. c/z$^\bullet$ ions from the top-down ECD of the 26+ charge state of denatured aldolase monomer are in red, b/y ions from the top-down CAD of the 26+ charge state of denatured aldolase are in green, and the c/z$^\bullet$ ions from the native top-down ECD of aldolase tetramer (entire charge state envelope without isolation) are in cyan.

The three-dimensional structure of the aldolase tetramer is shown in Figure 3. To compare the flexibility of the structure to the data from ECD of the aldolase tetramer, one of the subunits (B-chain) is presented as B-factor putty and the D-chain is shown with its native ECD backbone cleavage regions colored in red. The remaining A- and C-chains are shown in gray. Although the C-terminal region (AA 340−363) of each subunit is highly flexible based on the crystallography B-factor (see B-chain in Figure 3A), only 4 out of 75 backbone cleavage sites are from the AA 340−363 region. Instead, the native ECD fragments largely originate from surface regions of the protein structure (see D-chain in Figure 3A). The N-terminal regions are not directly involved in the interfaces between subunits, but they are located in regions that are partially buried, which is consistent with the limited c-ions observed. To better show the native ECD backbone cleavage regions, the D-chain is rotated 90 degrees clockwise (Figure 3B). It is clear that, although protein structure flexibility might play a role in the native top-down ECD fragmentation pattern, for aldolase the ECD cleavage sites are not limited to the flexible region. In addition, backbone cleavage regions from CAD (yellow) and ECD (cyan) of denatured aldolase are complementary with the native ECD results.

In summary, unit mass resolution measurements for a 158 kDa protein complex under native MS with high mass accuracy are demonstrated. The results demonstrate that with superior resolving power, mass accuracy, and versatile fragmentation

dx.doi.org/10.1021/ac4033214 | Anal. Chem. 2014, 86, 317−320

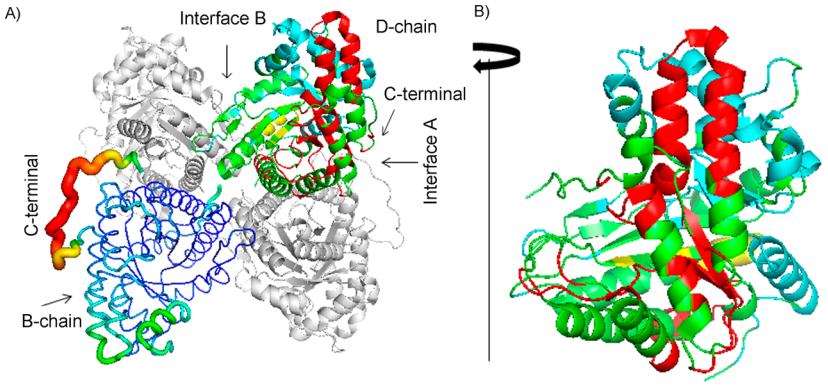

Figure 3. (A) Structure of tetrameric aldolase (1ZAH).[29] A- and C-chains are shown as gray ribbons, the B-chain is shown in B-factor putty, and the D-chain is in cartoon with native ECD cleavage sites colored in red, CAD cleavage sites of denatured aldolase in yellow, and ECD cleavage sites of the N-terminal region from ECD of denatured aldolase in cyan. (B) The D-chain is rotated 90 degrees clockwise to show the outer surface region of the subunit structure.

techniques, rich information related to the three-dimensional structure of protein complexes can be gathered by FTICR MS.

■ ASSOCIATED CONTENT

Ⓢ Supporting Information

Experimental details and additional information as noted in text. This material is available free of charge via the Internet at http://pubs.acs.org.

■ AUTHOR INFORMATION

Corresponding Author

*Phone: 310 794 7023. Fax: 310 206 4038. E-mail: JLoo@chem.ucla.edu.

Notes

The authors declare no competing financial interest.

■ ACKNOWLEDGMENTS

Support from the U.S. National Institutes of Health (Grants R01 GM103479 and S10 RR028893) and the U.S. Department of Energy (UCLA Institute of Genomics and Proteomics; Grant DE-FC03-02ER63421) are acknowledged.

■ REFERENCES

(1) Heck, A. J. R. *Nat. Methods* **2008**, *5*, 927−933.
(2) Lemaitre, J.-M.; Danis, E.; Pasero, P.; Vassetzky, Y.; Méchali, M. *Cell* **2005**, *123*, 787−801.
(3) Hilton, G. R.; Benesch, J. L. P. *J. R. Soc. Interface* **2012**, *9*, 801−816.
(4) Ge, Y.; Rybakova, I. N.; Xu, Q.; Moss, R. L. *Proc. Natl. Acad. Sci. U.S.A.* **2009**, *106*, 12658−12663.
(5) Mao, Y.; Valeja, S. G.; Rouse, J. C.; Hendrickson, C. L.; Marshall, A. G. *Anal. Chem.* **2013**, *85*, 4239−4246.
(6) Zhang, H.; Cui, W.; Wen, J.; Blankenship, R. E.; Gross, M. L. *Anal. Chem.* **2011**, *83*, 5598−5606.
(7) Geels, R. B. J.; van der Vies, S. M.; Heck, A. J. R.; Heeren, R. M. A. *Anal. Chem.* **2006**, *78*, 7191−7196.
(8) Xie, Y.; Zhang, J.; Yin, S.; Loo, J. A. *J. Am. Chem. Soc.* **2006**, *128*, 14432−14433.
(9) Clarke, D.; Murray, E.; Hupp, T.; Mackay, C. L.; Langridge-Smith, P. R. *J. Am. Soc. Mass Spectrom.* **2011**, *22*, 1432−1440.
(10) Valeja, S. G.; Kaiser, N. K.; Xian, F.; Hendrickson, C. L.; Rouse, J. C.; Marshall, A. G. *Anal. Chem.* **2011**, *83*, 8391−8395.
(11) Boldin, I. A.; Nikolaev, E. N. *Rapid Commun. Mass Spectrom.* **2009**, *23*, 3213−3219.
(12) Boldin, I. A.; Nikolaev, E. N. *Eur. J. Mass Spectrom.* **2008**, *14*, 1−5.
(13) Nakata, M. T.; Hart, G.; Peterson, B. *J. Am. Soc. Mass Spectrom.* **2010**, *21*, 1712−1719.
(14) Kelleher, N. L.; Senko, M. W.; Siegel, M. M.; McLafferty, F. W. *J. Am. Soc. Mass Spectrom.* **1997**, *8*, 380−383.
(15) Marshall, A. G.; Hendrickson, C. L.; Jackson, G. S. *Mass Spectrom. Rev.* **1998**, *17*, 1−35.
(16) Boldin, I. A.; Nikolaev, E. N. *Rapid Commun. Mass Spectrom.* **2011**, *25*, 122−126.
(17) Nikolaev, E. N.; Boldin, I. A.; Jertz, R.; Baykut, G. *J. Am. Soc. Mass Spectrom.* **2011**, *22*, 1125−1133.
(18) Nikolaev, E. N.; Vladimirov, G. N.; Jertz, R.; Baykut, G. *Mass Spectrom.* **2013**, *2*, 1−6.
(19) Mitchell, D. W.; Smith, R. D. *J. Mass Spectrom.* **1996**, *31*, 771−790.
(20) Nikolaev, E.; Boldin, I.; Jertz, R.; Baykut, G. *J. Am. Soc. Mass Spectrom.* **2011**, *22*, 1125−1133.
(21) Yergey, J.; Heller, D.; Hansen, G.; Cotter, R. J.; Fenselau, C. *Anal. Chem.* **1983**, *55*, 353−356.
(22) Qi, Y.; Barrow, M. P.; Li, H.; Meier, J. E.; Van Orden, S. L.; Thompson, C. J.; O'Connor, P. B. *Anal. Chem.* **2012**, *84*, 2923−2929.
(23) Qi, Y.; Thompson, C. J.; van Orden, S. L.; O'Connor, P. B. *J. Am. Soc. Mass Spectrom.* **2011**, *22*, 138−147.
(24) Xian, F.; Hendrickson, C. L.; Blakney, G. T.; Beu, S. C.; Marshall, A. G. *Anal. Chem.* **2010**, *82*, 8807−8812.
(25) Zubarev, R. A. *Mass Spectrom. Rev.* **2003**, *22*, 57−77.
(26) Wen, J.; Zhang, H.; Gross, M. L.; Blankenship, R. E. *Biochemistry* **2011**, *50*, 3502−3511.
(27) Yin, S.; Xie, Y.; Loo, J. A. *J. Am. Soc. Mass Spectrom.* **2008**, *19*, 1199−1208.
(28) Yin, S.; Loo, J. *J. Am. Soc. Mass Spectrom.* **2010**, *21*, 899−907.
(29) St-Jean, M.; Lafrance-Vanasse, J.; Liotard, B.; Sygusch, J. *J. Biol. Chem.* **2005**, *280*, 27262−27270.